2006 IEEE Nuclear Science Symposium Conference Record M11-212

Impact of Photon Transport Properties on the Detection Efficiency of Scintillator Arrays

Stefan Wirth, Wilhelm Metzger, Khanh Pham-Gia, Björn J. Heismann

***Abstract*–For spatially resolved X- and gamma ray detection pixelated scintillator arrays are used. In this study we simulate the quantum gain process of a scintillator array and its impact on the detective quantum efficiency of the detector system. The simulation tool comprises a full physical Monte-Carlo model of the X-ray interactions as well as the transport processes of the scintillation photons within the detector system. As an example, we analyze an Gd_2O_2S:Pr scintillator array with typical 1 mm pixel pitch and TiO_2 based reflective material.**

The results indicate that for integrating systems fluorescence escape effects play a major role in the noise performance of scintillating pixel detectors. Additionally, the light generation and transport processes can have an impact on the signal-to-noise ratio.

I. Introduction

Pixelated scintillator arrays are used for spatially resolved X- and gamma ray detection. Commonly, the pixel structure is defined by sawing gaps into the scintillator bulk and filling these gaps with a light reflective material. In case of an X-ray quantum absorption process in the scintillator material, a cloud of optical photons is created. These photons isotropically propagate within the scintillator pixel and are reflected diffusely at five of the six pixel walls. At the bottom side of the pixel volume a light sensor collects the transmitted photons.

In this study the impact of material parameter and geometry variations on basic detection properties like light yield, crosstalk or signal-to-noise ratio SNR is examined.

II. Simulation Framework

Our simulation tool comprises a full physical Monte-Carlo model of the X-ray interactions as well as the transport processes of the photons within the detector system.

For X-ray interaction, all major effects like absorption, scattering and escape fluorescence of X-ray quanta with energies of 20 keV up to 140 keV are taken into account. Incoming X-rays are either mono energetic or distributed according to typical tube emission spectra (see Fig 1). The conversion gain from X-ray energy deposit to optical photons is assumed as ε_{EC} = 0.12 with an uncertainty of $\sigma \approx 0.04$ relative to the mean energy loss.

Manuscript received November 10, 2006.

S. Wirth and B. J. Heismann are with Siemens Medical Solutions, Division Computed Tomography, Forchheim, Germany (e-mail: stefan.sw.wirth@siemens.com).

W. Metzger and K. Pham-Gia are with Siemens Corporate Technology, Division Materials & Microsystems, München, Germany

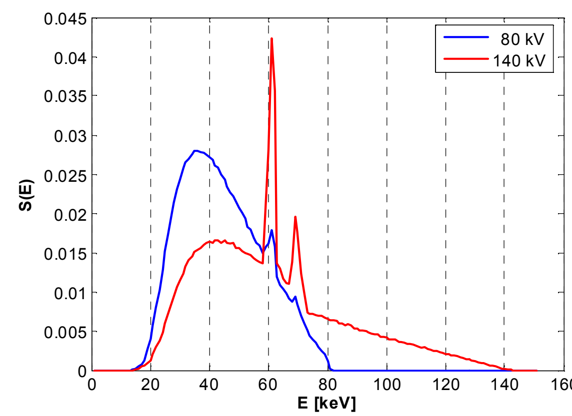

Fig. 1. Tube emission spectra S(E) for 80 and 140 kV X-ray tube voltage, tungsten anode, 2mm Al pre-filtering

The simulation of photon propagation covers both bulk interactions like scattering or reabsorption and effects at the pixel walls, which include diffuse or specular reflection, absorption and transmission to adjacent pixels (see Fig. 2). The propagation is traced in the entire detector system until the photons are absorbed, lost by leaving the detector system or detected at the photodiode array.

Basic parameters like scatter and absorption coefficients of the scintillator material as well as optical properties of the reflective materials (reflectivity, transmittance and absorption) are derived from experimental results.

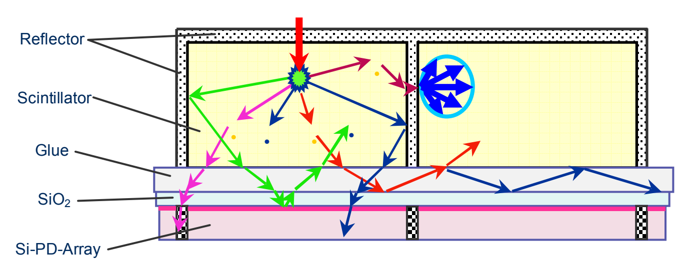

Fig. 2. Various effects of photon interaction within an array of scintillator and photodiode pixels

III. Detector Response Function

For a generalized analysis of the detector behavior the detector response was simulated for mono energetic X-ray input. The number of photons detected at the photodiode gives the output signal E' for each individual X-ray event. Thus, any effects of the photodiode and the subsequent electronics on signal quality are neglected. The resulting detector response function D(E',E) is shown in Fig. 3 for initial X-ray energies from 20 keV up to 140 keV and in Fig. 4 for specific input energies of 30, 50, 60 and 130 keV, respectively.

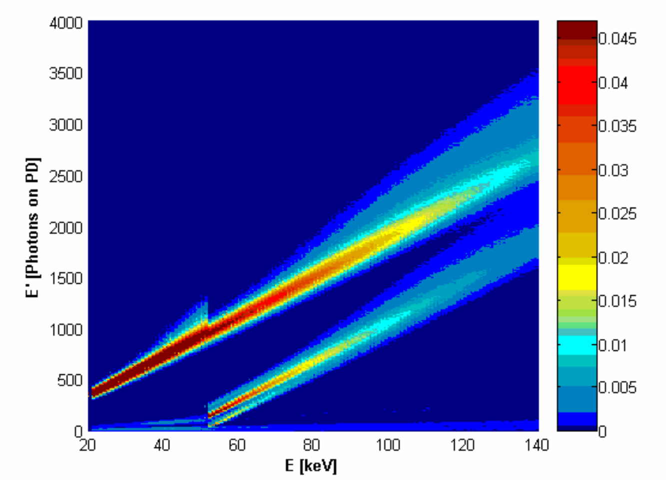

Fig. 3. Detector response function D(E',E); color coded probability, to detect E' photons at a given input energy E

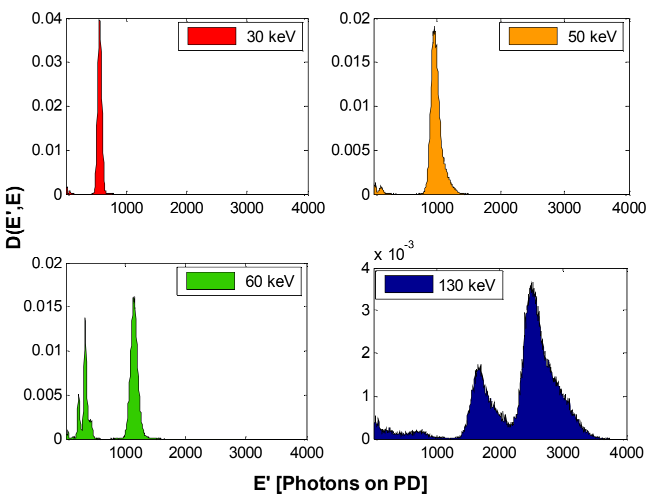

Fig. 4. Detector response function D(E',E) for fixed X-ray input energies E = 30, 50, 60 and 130 keV

Two major effects are visible which lead to a significant spread of the output signal:

- additional peaks due to the loss of K-escape quanta above 50 keV (Gd K-edge)
- signal tailing at higher energies due to higher light yield close to the photodiode

IV. Signal Analysis

In real applications the X-ray input spectrum is given by typical distributions S(E) as in Fig. 1. Therefore, the signal output distribution ξ(E') is given by:

$$\xi(E') = D(E',E) \cdot S(E)$$

Fig. 5 shows the calculated output distributions for a 140 kV input spectrum after passage through air or a 20 cm water phantom.

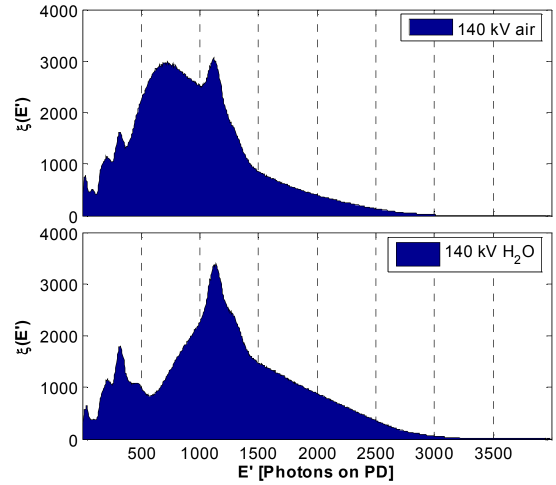

Fig. 5. Signal distribution ξ(E') for X-ray input spectra of 140 kV tube voltage for air and 20 cm water

The statistical evaluation of integrated signals shows a reduction of the signal-to-noise ratio in the input channel SNR_{in} of up to 3 % compared to the quantum statistical limit. The detection process within the scintillator gives a further reduction of 6 to 8 % for the SNR in the output channel SNR_{out} (see Fig. 6). SNR_{in} and SNR_{out} given by:

$$SNR_{in} = \frac{\left\langle \int E_N \, dN \right\rangle}{\sigma(\int E_N \, dN)} \qquad SNR_{out} = \frac{\left\langle \int E_N' \, dn \right\rangle}{\sigma(\int E_N' \, dn)}$$

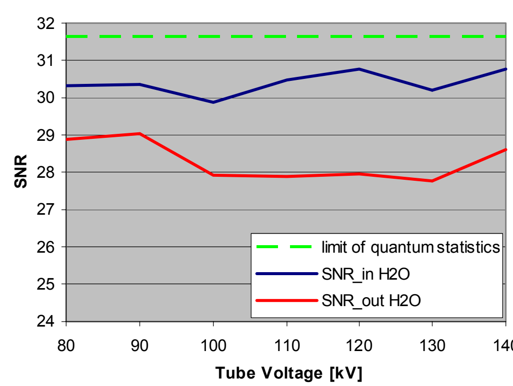

Fig. 6. SNR for integrated signals with N=1000±31 X-rays simulated.

V. Summary

The loss of K-escape quanta and photon transport mechanisms within a scintillator pixel mainly affect the composition of the output signal detected at the light sensor.

In integrating systems the SNR is dominated by the quantum statistics of the X-ray input flux. Due to the energy distribution in the X-ray spectra the SNR in the input channel is slightly reduced by up to 3 %. The detection process in the scintillator causes another moderate SNR reduction of 6 to 8 %.